Analytical and Bioanalytical Chemistry (2019) 411:4375–4382
https://doi.org/10.1007/s00216-019-01761-x

TRENDS

Electrochemiluminescence as emerging microscopy techniques

Alessandra Zanut[1] · Andrea Fiorani[2] · Sara Rebeccani[1] · Sagar Kesarkar[1] · Giovanni Valenti[1]

Received: 14 December 2018 / Revised: 30 January 2019 / Accepted: 6 March 2019 / Published online: 24 April 2019

Abstract

The use of electrochemiluminescence (ECL), i.e., chemiluminescence triggered by electrochemical stimulus, as emitting light source for microscopy is an emerging approach with different applications ranging from the visualization of nanomaterials to cell mapping. In this trend article, we give an overview of the state of the art in this new field with the purpose to illustrate all the possible applications so far explored as well as describing the mechanism underlying this transduction technique. The results discussed here would highlight the great potential of the combination between ECL and microscopy and how this marriage can turn into an innovative approach with specific application in analytical sciences.

Keywords Electrochemiluminescence · Electrochemical imaging · Biosensors · Immunoassay · Electrochemistry

Introduction

Electrochemically generated chemiluminescence or simply electrochemiluminescence (ECL) is a luminescent phenomenon induced by electrochemical stimulus. ECL is based on the electrochemical generation of species that undergo high-energy electron transfer reactions to form light-emitting excited states [1–4].

Since the first pioneering work from Bard and co-workers, the most used ECL dyes are Ru (II) polypyridine complexes, and in particular tris(2,2′-bipyridyl) ruthenium (II), $[Ru(bpy)_3]^{2+}$.

Thanks to the combination between electrochemical and spectroscopic methods, ECL possesses several advantages over chemiluminescence and photoluminescence, such as (*i*) superior temporal and spatial control on light emission, (*ii*) intrinsically very low background and high sensitivity (pmol L^{-1}) due to the absence of excitation light, and (*iii*) broad dynamic range (i.e., more than six order of magnitude) and rapid measurement (i.e., few seconds) with low volume (≤ 1 ml) [5–10].

In particular, ECL has been a great success, as transduction method, in different analytical field such as environmental investigations, bioanalysis [11], and immunoassays [12, 13], thanks to the unique signal to noise ratio also in real and very complex matrices such as cell lysates [14], urines, and blood [15]. As a matter of fact, ECL has become a powerful analytical technique widely studied and applied both from the academic and industrial point of view. If we have a look at the last 20 years, the number of scientific publications focused on ECL research activity has been exponentially increasing (see Fig. 1a) reaching almost 3000 publications per year in 2018.

Regarding the industrial field, the first ECL commercial analyzer was produced by IGEN International in 1994. Nowadays, Roche Diagnostic commercialize a clinical analyzer, Elecsys®, optimized for more than 150 immunoassays based on ECL technologies [17]. Another important ECL analyzer is commercialized by Meso Scale Discovery and is focused on the multiplexing analysis [18].

Recently, Dropsense started the implementation of portable device that combine ECL with screen-printed electrode [19]. Although many mechanisms for the signal generation have been proposed, the so-called *oxidative reduction* based on tripropyl amine (TPrA) as sacrificial coreactant is the most used. This is the case in which the dye is not free to diffuse, because constricted in close proximity to the electrode surface,

Published in the topical collection *Young Investigators in (Bio-)Analytical Chemistry* with guest editors Erin Baker, Kerstin Leopold, Francesco Ricci, and Wei Wang.

✉ Giovanni Valenti
g.valenti@unibo.it

[1] Department of Chemistry "G. Ciamician", University of Bologna, Via F. Selmi 2, 40126 Bologna, Italy

[2] Department of Chemistry, Keio University, 3−14−1 Hiyoshi, Yokohama 223−8522, Japan

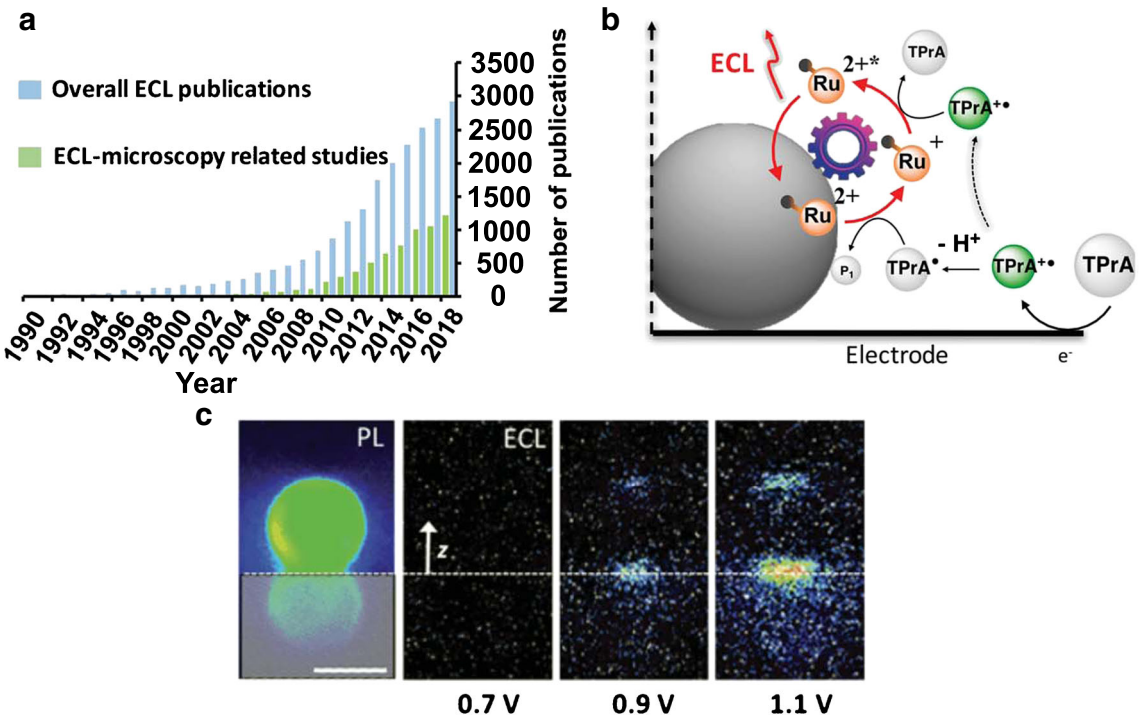

Fig. 1 **a** Collected statistics of published research papers on ECL (blue) and ECL microscopy (green) (from 1990 to 2018). Datas obatained from Scopus, 1 November 2018. **b** Schematic representation of ECL heterogeneous mechanism for $[Ru(bpy)_3]^{2+}$/TPrA. Ru^{2+} is $[Ru(bpy)_3]^{2+}$, Ru^{+} is $[Ru(bpy)_3]^{3+}$, $Ru^{2+}*$ is $[Ru(bpy)_3]^{2+}*$ and TPrA is *tripropyl amine*. **c** Side-view images of a 12 mm PS bead labeled with the ruthenium complex. The first image is obtained by PL and the following ones by ECL in a PBS solution containing 100 mM TPrA (pH = 7.4). The dashed line shows the position of the GC electrode surface and the blurred zone below represents the PL reflection on the electrode surface. Scale bar, 10 mm. Reproduced from Ref. [16], copyright 2018, with permission of Royal Society of Chemistry

and the ECL emission is triggered by TPrA oxidation to radical cation ($TPrA^{\bullet+}$) at an applied potential higher than 0.88 V (vs Ag/AgCl see Fig. 1b).

Briefly, the determining step in this kind of ECL mechanism is the chemical reaction that follow the TPrA oxidation and the lifetime of $TPrA^{\bullet+}$. In fact, $TPrA^{\bullet+}$ is highly instable and undergo to further deprotonation to $TPrA^{\bullet}$, a strong reductant (Eq. 3). The latter radical reduces $Ru(bpy)_3^{2+}$ to $Ru(bpy)_3^{+}$ (Eq. 4) while pristine $TPrA^{\bullet+}$ oxidizes $Ru(bpy)_3^{+}$ to generate the excited state $Ru(bpy)_3^{2+}*$ (Eq. 5). The crucial part of this mechanism is the compresence in the diffusion layer of both radical and radical cation of TPrA. Finally, the $Ru(bpy)_3^{2+}*$ relaxes to the ground state generating the ECL signal [20, 21].

$$TPrAH^{+} \leftrightarrows TPrA + H^{+} \quad (1)$$

$$TPrA - e \leftrightarrows TPrA^{\bullet+} \quad (2)$$

$$TPrA^{\bullet+} \leftrightarrows TPrA^{\bullet} + H^{+} \quad (3)$$

$$TPrA^{\bullet} + Ru(bpy)_3^{2+} \leftrightarrows P1 + Ru(bpy)_3^{+} \quad (4)$$

$$TPrA^{\bullet+} + Ru(bpy)_3^{+} \leftrightarrows TPrA + Ru(bpy)_3^{2+*} \quad (5)$$

$$Ru(bpy)_3^{2+}* \rightarrow Ru(bpy)_3^{2+} + hv \quad (6)$$

where P1 is the product of the homogeneous $TPrA^{\bullet}$ oxidation.

In the recent years, an important breakthrough in the development of analytical ECL devices and applications is the combination of this transduction technique with microscopy (see green histogram in Fig. 1a). With this approach, the high signal to noise ratio is implemented with the spatial resolution intrinsic in the ECL techniques. Up to now, there is no commercially available instrumentation for ECL imaging but the typical laboratory setup for this type of technique includes an epifluorescence microscope connected to a potentiostat and a CCD camera.

In this context, Amatore [22] and Bard [23] pioneeringly combined the microscopy with ECL in order to observe spatial resolution concentration profiles of species generated in the proximity of the electrode surface. After them, much progress has been made until recent times, when our research group reported the application of ECL microscopy for the visualization of single micrometric beads [24]. The strategy

used, schematized in Fig. 1b, is based on the immobilization of an ECL active dye on the beads surface and the indirect activation of ECL emission by the electrogenerated radicals of an appropriate sacrificial coreactant, typically TPrA. According to the aforementioned mechanism, the diffusion and stability of coreactant radicals play a crucial role in determining, at each position of the microobject surface, the signal intensity and its time evolution.

A mapping of ECL reactivity and of the emission spatial distribution was reported by Sojic and co-workers [16]. They showed that the maximum of ECL emission occurs in the micrometric region where concentrations of $TPrA^{\bullet}$ and $TPrA^{\bullet+}$ radicals are locally the highest. They also demonstrated by analyzing the beads lateral image that only the luminophores located within the 3 μm region close to the electrode contribute to the ECL signal as it is shown in Fig. 1c. Those fundamental research investigations open the prospective for the combination between ECL and microscopy for the surface-confined mapping and quantification of different analytes. In this article, we highlight the recent advances of ECL microscopy applied for the visualization of micrometric and sub-micrometric objects. Future challenges and research trends will be also pointed out along with the discussion.

ECL imaging for sensor application

Because of very high sensitivity, good selectivity, insensitivity to matrix effects, and high dynamic range, ECL is a robust sensing methodology.

The majority of ECL detection systems involve the $Ru(bpy)_3^{2+}$ luminophore or its derivates and TPrA as co-reactant especially for the fact that this mechanism allows the generation of ECL in heterogeneous systems. The analytical application is based on the fact that ECL intensity is proportional to the concentration of the ECL luminophore attached to a sensing element of interest (protein, DNA, antibodies, etc) or to the concentration of coreactant, depending on the case. If ECL experiments are carried out in the presence of high and constant concentration of coreactant, the signal intensity will linearly depend on the concentration of ECL emitter in a wide dynamic range. Remarkably, recent achievements in nanoscience and nanotechnology have demonstrated the potential for improving greatly both the sensitivity and selectivity of electrochemiluminescent sensors and biosensors. In fact, a sensor platform can be miniaturized to a size less than 1 μm offering advantages in terms of increased sensitivity and compactness. Sentic et al. exploited different types of nanoelectrode array (NEAs) with precisely controlled geometries to map the ECL behavior at different concentration of coreactant through imaging technique (see Fig. 2a) [25]. NEAs were fabricated by e-beam lithography on a polycarbonate layer deposited on boron-doped diamond (BDD) substrates exposing to the solution electrodes with different dimensions and inter-electrode distances. The attractiveness of such nanostructured systems resides also in the possibility to functionalize with biomolecules of interest the dielectric surface surrounding each nanoelectrode, instead of on the electrode itself; therefore, it may result easier to combine the highly specific molecular recognition mechanisms with high sensitivity (low detection limits).

As a matter of fact, a large number of biomolecules such as proteins, DNAs, and peptides have no co-reactant functionalities, or they can give very poor ECL signal. Thus, their ECL detections are mainly carried out with solid phase ECL assay formats in which biomolecules linked with ECL labels, are immobilized on a solid substrate and ECL is generated in the presence of a co-reactant, typically TPrA [27].

In this context imaging techniques prove to be very useful for the visualization of antigens of interest immobilized or selectively captured on solid sensing platform. For this purpose, the sandwich format is the most used based on recognition properties and antibody/antigen binding. Deiss et al. exploited this system to functionalize array of microspheres with different antibodies in order to detect specific molecules of interest through a biotinylated detection antibody that was finally attached to streptavidin-modified $Ru(bpy)_3^{2+}$ as ECL label [28]. The ECL response of the beads on the platform was recorded with a CCD camera thus enables the simultaneous imaging of each sensing beads in the array.

One general drawback of immunoassays is that multiple operations to load samples, add reagents to block nonspecific binding, remove interferences, and detect target proteins are needed and this greatly limits their use as point-of-care systems. This problem could be solved with the use of microfluidic devices integrated with the ECL imaging setup. The integration of components into low-cost and fully automated devices is of great interest and represents a current challenge in research that will bring a great improvement in the field of medical sciences. In this context, in recent years, Rusling and co-workers proved to be a pioneer, in fact, they investigate the effect of the electrode and inter-electrode distances dimensions; they understood that the detection of light with a camera must be integrated into the chip space and had the intuition of combining this information with a microprocessor-controlled automatic microfluidic for simultaneous multiplex detection of small panels proteins using ECL imaging [29].

The reported device consists of microfluidic channels precision cut from silicone gaskets, containing single-wall carbon nanotubes (SWCNT) functionalized with capture antibodies, placed between two PMMA plates fitted with optically clear

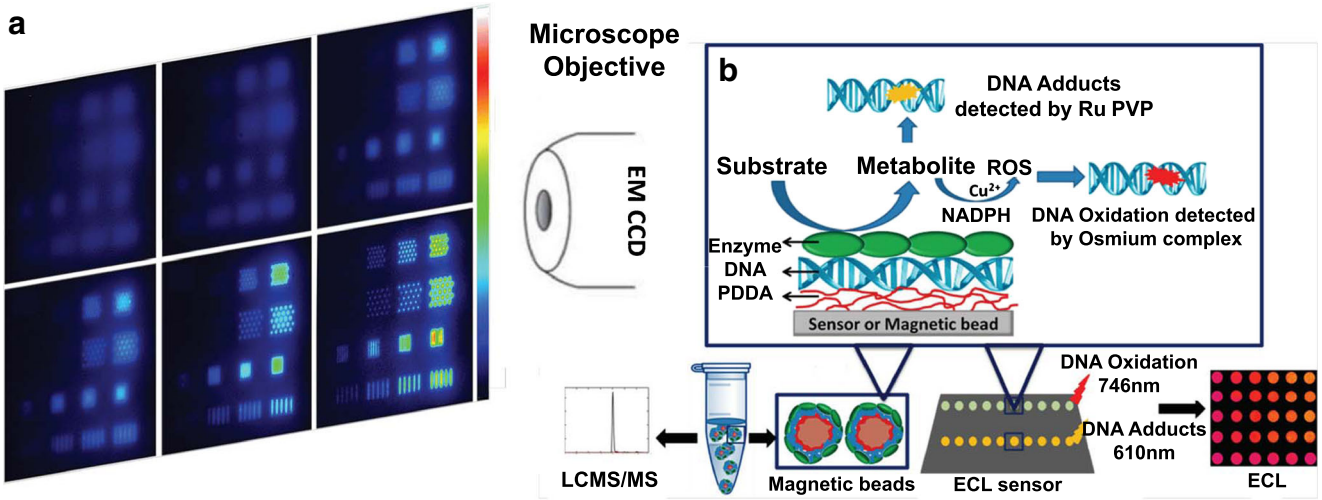

Fig. 2 **a** ECL images of the NEAs obtained with a constant concentration of Ru $(bpy)_3^{2+}$ and increasing concentrations of TPrA (1–85 mM). Images were recorded in the dark with a × 50 objective when applying a constant potential of 1.2 V vs. Ag/AgCl/KCl. Reproduced from Ref. [25], copyright 2018, with permission of Springer Nature. **b** Array strategy for screening genotoxic pathways using DNA/enzyme films with ECL imaging readout . Reproduced from Ref. [26], copyright 2018, with permission of Royal Society of Chemistry

acrylic windows above each microwell channel to pass ECL light to a CCD camera enable imaging. The same type of technology was also used to detect, for the first time, oxidized DNA [26]. In this case, as transduction strategy, ECL-producing osmium complexes with electrocatalytic pathways that employ 8-oxodG in DNA as a coreactant has been used.

An improvement of this device using immunoarray and ECL transduction scheme is reported the following year by presenting a supercapacitor-powered electrochemiluminescent (ECL) protein immunoarray fabricated by an inexpensive 3-dimensional(3D)printer [30]. These arrays use light-activated super capacitors to generate ECL that is captured with a CCD camera.

The exciting feature of the ECL lies in the fact that this technique has found its applicability even before knowing in a precise way the mechanisms that generate it, especially in close proximity to the electrode. This is why, especially ECL imaging proves to be a very useful tool to investigate the mechanisms that generate ECL at the micro and nanometric level.

ECL imaging at nanoscale

The electrochemical imaging at nanoscale level is a rapidly growing field with many important applications [31]. Although different successful approach has been presented to amplify the small current characteristic of single nanomaterial, experimental difficulties are generally associated in measuring very small currents or changes. Regarding this, thanks to the very high signal to noise ratio, ECL can be an emerging transduction technique for single nanomaterial characterization. Bard and co-workers showed the way to observe single particle collision with ECL [32, 33]. In their approach, the catalytic propriety of the nanoparticles towards the coreactant oxidation induces an ECL generation for each nanoparticles collision. In this case, the ECL emission intensity and the frequency could be correlated with the nanomaterial dimension and concentration. Similar approach has been used by Willets and coworkers for the visualization of gold nanowires deposited on ITO electrode [34]. Also in this case, the differences in the coreactant oxidation kinetics between gold and ITO allow the ECL emission only in correspondence of the nanomaterial. Finally, Pan and colleagues visualized for the first time local redox activity at the single gold nanoparticle level [35]. They were able to map the ECL intensity and correlate with the nanoparticle size from 30 to 300 nm.

ECL imaging for cells

ECL as transduction method for imaging biological sample such as cell and tissue is a very recent approach but has already produced a significant amount of publications.

Compared to main imaging strategy such as fluorescent labeling (using GFP or small molecule fluorophores) or luminescence (luciferin-based assay), ECL detection of single living cells proved to be a new method to study the surface chemical composition and local activities of cells with high signal to noise ratio. In fact, the first two techniques mentioned possess some intrinsic limitations related to the interaction of light with microscopic components of tissues. Moreover, ECL imaging does not require any filtering

strategies that represent the major fundamental limitation in the detection of fluorophores.

The main strategy for the ECL imaging of single cells is based on adherent cells cultured directly on the electrode allowing high analysis throughput with high spatial resolution and low detection limit.

Research so far has focused on two fronts, first on the visualization and quantification of molecules present inside the cell and almost in parallel, on the visualization of cellular surface structures.

Xu et al. reported for the first time the ECL from luminol to analyze intracellular molecules, such as glucose, at single cells level [36]. The luminol/H_2O_2 system has a wide application since hydrogen peroxide is often released by the cell as a result of various intra- and extracellular biochemical processes. In this work, the individual cells were retained in cell-sized microwells on a gold-coated indium tin oxide (ITO) slide and treated with triton X-100 in order to break the cellular membrane releasing intracellular glucose that react with glucose oxidase to generate hydrogen peroxide and thus luminol luminescence under positive potential (see Fig. 3a). Similar achievement has been recently reached by Jiang and co-workers who reported the optimization of an ECL biosensor for in situ monitoring of H_2O_2 released from Hela cells using 3D porous structured conductive Hydrogel [39].

Although in this work imaging is not used as a detection technique, the use of biocompatible conductive hydrogels makes cell adhesion much easier and, thanks to its 3D structure, proves to be useful in the study of the behavior of ECL signals in complex systems such as body tissues.

Moreover, they can overcome the steric hindrance that occurs when cells are adherent on the electrode surface. This property has been used also by Liu et al. to analyze the H_2O_2 released from cells at the single-cell level overcoming the hindrance effect using chitosan and nano-TiO_2 modified fluoride-doped tin oxide conductive glass [40].

In all these research works, the use of microelectrode arrays as panel for ECL analysis represents a limit to single-cell imaging. Having the possibility to exploit molecules present on the cell membrane for the generation of ECL signals has exceeded this limit.

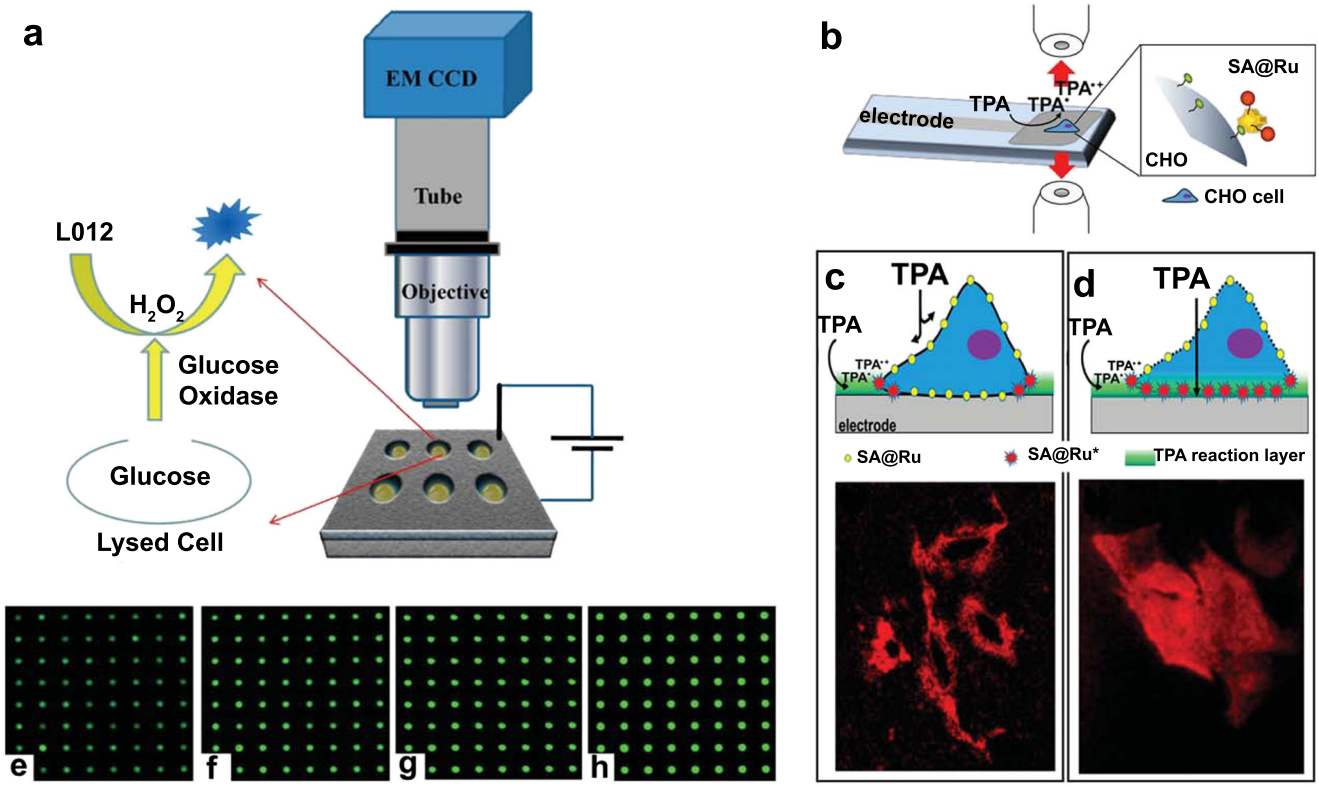

Fig. 3 **a** Schematic electrochemiluminescence imaging setup for fast analysis of intracellular glucose at single cells together with ECL imaging of aqueous hydrogen peroxide at ITO/microwell regions in 10 mM PBS with 200 μM L012 adding different concentration (5–500 μM). Reproduced from [36], copyright 2018, with permission of American Chemical Society, **b** schematic representation of the strategy used to attach Ru labels to the biotinylated proteins of the cellular membrane and ECL imaging. TPA diffusion through the cell membrane and resulting localization of the ECL-emitting regions in **c** fixed Chinese hamster ovary (CHO) cells reproduced from [37], copyright 2018, with permission of America Chemical Society, and **d** also permeabilized obtained in the transmission configuration through the CNT inkjet-printed electrode. Reproduced from [38], copyright 2018, with permission of America Chemical Society

Zhou and colleagues explained how they obtained luminol electrochemiluminescence imaging of active membrane cholesterol at single living cells [41]. The peculiarity of this work lies in the fact that the generation of the ECL signal exploits an intrinsic property of a molecule of interest. Therefore, signal discrimination takes place, thanks to some molecules, such as cholesterol, which have a higher chemical activity allowing the generation of the ECL signal. With this approach, it is not possible to obtain information on the structure of the cell surface, but only on the lower part of the cell, in close proximity to the electroactive material.

We, in collaboration with Sojic group, recently reported for the first time a spatially resolved ECL imaging of single cells where their membrane proteins were labeling with Ru $(bpy)_3^{2+}$. Using immunochemistry strategies, important biomarkers on the surface of cancer cells could be imaged with high spatial resolution and signal to noise ratio [37]. We observed that ECL was not emitted by the entire cell surface but just at the cell borders leaving out the internal regions of the cell where luminophores can be located too far (some micrometers) from the electrode surface (see the comparison in Fig. 3b between green and red image). In fact, heterogeneous ECL is intrinsically a surface-confined process and it is limited by the access of the electrogenerated radicals to the luminophore site, explaining the observed phenomenon.

Recently, we also use different protocols in order to permeabilized the cell and enable the access to the TPrA radicals and therefore generate ECL even in the internal areas of the cell (Fig. 3c) [38]. Also in this case, the ECL emission is restricted to the immediate vicinity of the electrode surface, but thanks to the permeabilization the basal membrane is ECL active and together with ECL microscopy reveals details, which are hardly resolved by classic fluorescence techniques.

Outlook

Electrochemiluminescence is one of the leading transduction techniques in analytical chemistry ranging from success industrial application to the advanced analytical quantification. Coupling ECL with microscopy reveals a promising new approach for the quantification and map of different analytes ranging from proteins to DNA. In this trends article, we have highlighted the emerging ECL imaging analytical and bioanalytical application and compared it with the most used imaging techniques (briefly resumed in a pratical decision table, Fig. 4). We reported examples of ECL microscopy applied in the developing of advanced biosensor in order to perform simultaneous multiplexing analysis. The application of ECL microscopy at nanoscale level visualization is well advanced and very high lateral resolution is already achieved. In this field with ECL, it is possible to visualize nanomaterials without illumination source or scanning probe techniques. Finally, the research on ECL-based microscopy from single cells mapping is just at the beginning but it will have important application in the extracellular and intracellular analysis. We have described how ECL microscopy has been used successfully and innovatively applied in several fields of research up to more recent applications that lays the groundwork for the ECL to become an in vitro imaging technique and

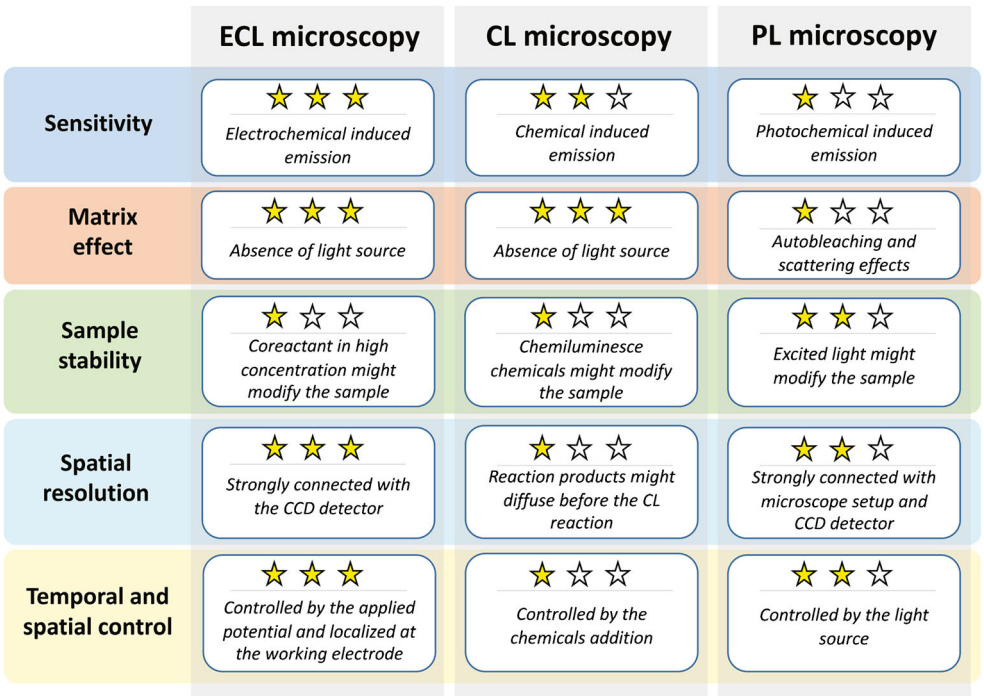

Fig. 4 Decision table showing the comparison between electro-, chemi-, and photoluminescence microscopy (ECL, CL, and PL respectively)

hopefully in vivo in the future. However, there are still many challenges that this technique is currently facing. In fact, thanks to the high sensitivity coupled with signal amplification, ECL imaging could significantly improve the signal to noise ratio thus allowing the detection of biomolecules at very low concentration. Most of the efforts are focus on the development of new dye-doped nanomaterial such as quantum dots [42] or dye-doped nanoparticles [43]. Moreover, since in ECL the electrode and the target are required to be in close proximity, the design of nanostructured electrodes capable to increase the surface stability and increase the rate of coreactant oxidation, it is certainly one of the key challenges that research is facing.

One important thing to underline is that the application of ECL microscopy as an analytical technique allows us not only to identify molecules or structures of interest but also to do active research on the mechanisms that regulate this transduction technique, which we are not still fully aware. There is still a huge room for improvement, and we believe that the research in this field will continue to grow exponentially. Above all, there is the need to develop biocompatible methods and coractants with features that enable to work in aqueous solution and most importantly, coractants with higher lifetimes in order to increase the ECL spatial yield and thus expand the emission layer.

All this features will be fundamental to turn ECL microscopy into a more efficient analytical tool.

Funding information We thank the University of Bologna, Italian Ministero dell'Istruzione, Università della Ricerca (FIRB RBAP11C58Y, PRIN-2010N3T9M4), FARB, Fondazione Cassa di Risparmio in Bologna.

Compliance with ethical standards

Conflict of interest The authors declare that they have no conflict of interest.

References

1. Bard JA, editor. Electrogenerated chemiluminescence. New York: Marcel Dekker; 2004.
2. Richter MM. Electrochemiluminescence (ECL). Chem Rev. 2004;104:3003–36.
3. Hesari M, Ding Z. Review—electrogenerated chemiluminescence: light years ahead. J Electrochem Soc. 2016;163:H3116–31.
4. Valenti G, Fiorani A, Li H, Sojic N, Paolucci F. Essential role of electrode materials in electrochemiluminescence applications. ChemElectroChem. 2016;3:1990–7.
5. Forster JR, Bertoncello P, Keyes TE. Electrogenerated chemiluminescence. Annu Rev Anal Chem. 2009;2:359–85.
6. Miao W. Electrogenerated chemiluminescence and its biorelated applications. Chem Rev. 2008;108:2506–53.
7. Gross EM, Durant HE, Hipp KN, Lai RY. Electrochemiluminescence detection in paper-based and other inexpensive microfluidic devices. ChemElectroChem. 2017;4:1594–603.
8. Li L, Chen Y, Zhu J-J. Recent advances in electrochemiluminescence analysis. Anal Chem. 2017;89:358–71.
9. Liu Z, Qi W, Xu G. Recent advances in electrochemiluminescence. Chem Soc Rev. 2015;44:3117–42.
10. Bertoncello P, Ugo P. Recent advances in electrochemiluminescence with quantum dots and arrays of nanoelectrodes. ChemElectroChem. 2017;4:1663–76.
11. Gross EM, Maddipati SS, Snyder SM. A review of electrogenerated chemiluminescent biosensors for assays in biological matrices. Bioanal. 2016;8:2071–89.
12. Huo X, Liu X, Liu J, Sukumaran P, Alwarappan S, Wong DKY. Strategic applications of nanomaterials as sensing platforms and signal amplification markers at electrochemical immunosensors. Electroanal. 2016;28:1730–49.
13. Rusling JF. Low-cost microfluidic arrays for protein-based cancer diagnostics using ECL detection. Interface Mag. 2016;25:47–51.
14. Juzgado A, Soldà A, Ostric A, Criado A, Valenti G, Rapino S, et al. Highly sensitive electrochemiluminescence detection of a prostate cancer biomarker. J Mater Chem B. 2017;5:6681–7.
15. Stewart AJ, Hendry J, Dennany L. Whole blood electrochemiluminescent detection of dopamine. Anal Chem. 2015;87:11847–53.
16. Sentic M, Milutinovic M, Kanoufi F, Manojlovic D, Arbault S, Sojic N. Mapping electrogenerated chemiluminescence reactivity in space: mechanistic insight into model systems used in immunoassays. Chem Sci. 2014;5:2568–72.
17. Roche Diagnostics Corp. 2018. www.roche.com
18. Meso Scale Discovery. 2018. www.mesoscale.com/en/technical_resources/our_technology/multi-array
19. Neves MMPS, González-García MB, Hernández-Santos D, Fanjul-Bolado P. A miniaturized flow injection analysis system for electrogenerated chemiluminescence−based assays. ChemElectroChem. 2017;4:1686–9.
20. Miao W, Choi JP, Bard AJ. Electrogenerated chemiluminescence 69: the Tris(2,2′-bipyridine) ruthenium (II), (Ru (bpy)32+)/tri-n-propylamine (TPrA) system revisited - a new route involving TPrA+ cation radicals. J Am Chem Soc. 2002;124:14478–85.
21. Daviddi E, Oleinick A, Svir I, Valenti G, Paolucci F, Amatore C. Theory and simulation for optimising electrogenerated chemiluminescence from Tris(2,2′-bipyridine)-ruthenium (II)-doped silica nanoparticles and tripropylamine. ChemElectroChem. 2017;4:1719–30.
22. Amatore C, Pebay C, Servant L, Sojic N, Szunerits S, Thouin L. Mapping electrochemiluminescence as generated at double-band microelectrodes by confocal microscopy under steady state. ChemPhysChem. 2006;7:1322–7.
23. Zu Y, Ding Z, Zhou J, Lee Y, Bard AJ. Scanning optical microscopy with an electrogenerated chemiluminescent light source at a nanometer tip. Anal Chem. 2001;73:2153–6.
24. Valenti G, Zangheri M, Sansaloni SE, Mirasoli M, Penicaud A, Roda A, et al. Transparent carbon nanotube network for efficient electrochemiluminescence devices. Chem Eur J. 2015;21:12640–5.
25. Sentic M, Virgilio F, Zanut A, Manojlovic D, Arbault S, Tormen M, et al. Microscopic imaging and tuning of electrogenerated chemiluminescence with boron-doped diamond nanoelectrode arrays. Anal Bioanal Chem. 2016;408:7085–94.
26. Bist I, Bhakta S, Jiang D, Keyes TE, Martin A, Forster RJ, et al. Evaluating metabolite-related DNA oxidation and adduct damage from aryl amines using a micro fl uidic ECL array. Anal Chem. 2017;89:12441–9.
27. Xu L, Li Y, Wu S, Liu X, Su B. Imaging latent fingerprints by electrochemiluminescence. Angew Chem Int Ed. 2012;51:8068–72.
28. Deiss F, LaFratta CN, Symer M, Blicharz TM, Sojic N, Walt DR. Multiplexed sandwich immunoassays using electrochemiluminescence imaging resolved at the single bead level. J Am Chem Soc. 2009;131:6088–9.

29. Kadimisetty K, Malla S, Sardesai NP, Joshi AA, Faria RC, Lee NH, et al. Automated multiplexed ecl immunoarrays for cancer biomarker proteins. Anal Chem. 2015;87:4472–8.
30. Kadimisetty K, Mosa IM, Malla S, Satterwhite-Warden JE, Kuhns TM, Faria RC, et al. 3D-printed supercapacitor-powered electrochemiluminescent protein immunoarray. Biosens Bioelectron. 2016;77:188–93.
31. Bentley CL, Edmondson J, Meloni GN, Perry D, Shkirskiy V, Unwin PR. nanoscale electrochemical mapping. Anal Chem. 2018;91:84–108.
32. Fan FRF, Bard AJ. Observing single nanoparticle collisions by electrogenerated chemiluminescence amplification. Nano Lett. 2008;8:1746–9.
33. Fan FRF, Park S, Zhu Y, Ruoff RS, Bard AJ. Electrogenerated chemiluminescence of partially oxidized highly oriented pyrolytic graphite surfaces and of graphene oxide nanoparticles. J Am Chem Soc. 2009;131:937–9.
34. Wilson AJ, Marchuk K, Willets KA. Imaging electrogenerated chemiluminescence at single gold nanowire electrodes. Nano Lett. 2015;15:6110–5.
35. Pan S, Liu J, Hill CM. Observation of local redox events at individual au nanoparticles using electrogenerated chemiluminescence microscopy. J Phys Chem C. 2015;119:27095–103.
36. Xu J, Huang P, Qin Y, Jiang D, Chen HY. Analysis of intracellular glucose at single cells using electrochemiluminescence imaging. Anal Chem. 2016;88:4609–12.
37. Valenti G, Scarabino S, Goudeau B, Lesch A, Jović M, Villani E, et al. Single cell electrochemiluminescence imaging: from the proof-of-concept to disposable device-based analysis. J Am Chem Soc. 2017;139:16830–7.
38. Voci S, Goudeau B, Valenti G, Lesch A, Jovic M, Rapino S, et al. Surface-confined electrochemiluminescence microscopy of cell membranes. J Am Chem Soc. 2018;140:14753–−14760.
39. Jiang X, Wang H, Yuan R, Chai Y. Functional three-dimensional porous conductive polymer hydrogels for sensitive electrochemiluminescence in situ detection of H2O2Released from live cells. Anal Chem. 2018;90:8462–9.
40. Liu G, Ma C, Jin BK, Chen Z, Zhu JJ. Direct electrochemiluminescence imaging of a single cell on a chitosan film modified electrode. Anal Chem. 2018;90:4801–6.
41. Zhou J, Ma G, Chen Y, Fang D, Jiang D, Chen HY. Electrochemiluminescence imaging for parallel single-cell analysis of active membrane cholesterol. Anal Chem. 2015;87:8138–43.
42. Jie G, Yuan J. Novel magnetic Fe 3O 4@CdSe composite quantum dot-based electrochemiluminescence detection of thrombin by a multiple DNA cycle amplification strategy. Anal Chem. 2012;84:2811–7.
43. Valenti G, Rampazzo E, Bonacchi S, Petrizza L, Marcaccio M, Montalti M, et al. Variable doping induces mechanism swapping in electrogenerated chemiluminescence of Ru (bpy)32+ Core − Shell silica nanoparticles. J Am Chem Soc. 2016;138:15935–42.